

# Modelling the effect of individual hearing impairment on sound localisation in sagittal planes

ROBERT BAUMGARTNER<sup>\*</sup>, PIOTR MAJDAK, AND BERNHARD LABACK

*Acoustics Research Institute, Austrian Academy of Sciences, Austria*

Normal-hearing (NH) listeners use monaural spectral cues to localize sound sources in sagittal planes, including up-down and front-back directions. The salience of monaural spectral cues is determined by the spectral resolution and the dynamic range of the auditory system. Both factors are commonly degraded in impaired auditory systems. In order to simulate the effects of outer hair cell (OHC) dysfunction and loss of auditory nerve (AN) fibres on localisation performance, we incorporated a well-established model of the auditory periphery [Zilany *et al.*, 2014, *J. Acoust. Soc. Am.* 135] into a recent model of sound localisation in sagittal planes [Baumgartner *et al.*, 2014, *J. Acoust. Soc. Am.* 136]. The model was evaluated for NH listeners and then applied on conditions simulating various degrees of OHC dysfunction. The predicted localisation performance is hardly affected by a moderate OHC dysfunction but drastically degrades in case of a severe OHC dysfunction. When further applied on conditions simulating loss of AN fibres with specific spontaneous rates (SRs), predicted localisation performance degrades if only high-SR fibres are preserved.

## INTRODUCTION

Monaural spectral cues enable sound localisation where binaural cues are ambiguous. This ambiguity occurs approximately in planes orthogonal to the interaural axis, the sagittal planes, and thus concerns localisation of both up-down and front-back directions. The mapping of direction-dependent spectral cues to perceived spatial direction is considered as being implemented in the auditory system as a comparison process between the incoming sound spectrum and learned spectral templates.

The extraction of spectral localisation cues relies on a proper functioning of the auditory periphery. Sensorineural hearing loss is known to degrade localisation performance especially within the sagittal planes (Otte *et al.*, 2013; Rakerd *et al.*, 1998). Degradation of localisation performance with high-frequency attenuation is relatively well understood (Baumgartner *et al.*, 2014; Best *et al.*, 2005), but is not sufficient to accurately explain individual localisation performance of hearing-impaired listeners (Noble *et al.*, 1994). Additional deficits that potentially affect localisation performance are a dysfunction of olivocochlear efferents for modulation of outer hair cell (OHC) activity causing broadened auditory filters (May *et al.*, 2004) as well as a noise-induced loss of auditory nerve (AN) fibres with low to moderate spontaneous

---

<sup>\*</sup>Corresponding author: robert.baumgartner@oeaw.ac.at

firing rates (SRs) resulting in a reduced dynamic range of AN responses (Furman *et al.*, 2013). These deficits are, however, hard to assess and quantify for real listeners.

In order to better understand the effect of peripheral deficits on localisation performance in the sagittal planes, this study aimed at simulating their consequences by means of an auditory model. To this end, we integrated a model of the auditory periphery (Zilany *et al.*, 2009; 2014) into a model of sound localisation in sagittal planes (Baumgartner *et al.*, 2014). First, we evaluated the modified model for normal-hearing listeners, and then, investigated effects of OHC dysfunctions and loss of specific SR fibres at various sound pressure levels (SPLs).

## **METHODS**

We use the interaural-polar coordinate system to describe auditory localization. The lateral angle in the horizontal plane ranges from  $-90^\circ$  at the left hand side to  $90^\circ$  at the right hand side. The polar angle in the sagittal plane ranges from  $-90^\circ$  to  $270^\circ$  with  $0^\circ$  corresponding to the front,  $90^\circ$  to the top, and  $180^\circ$  to the back of the listener.

### **Sagittal-plane localisation model**

The model from Baumgartner *et al.* (2014) follows a template-based comparison procedure. First, the incoming sound and the template head-related transfer functions (HRTFs) are processed by an approximation of the auditory periphery in order to obtain internal excitation patterns. Then, across-frequency differentiation with 1-equivalent-rectangular-bandwidth spacing and restriction to positive gradients yields gradient profiles. This gradient extraction is a functional approximation of the rising spectral edge sensitivity observed in the dorsal cochlear nucleus of cats (Reiss and Young, 2005). The incoming sound is, then, compared to the template HRTFs on the basis of the corresponding gradient profiles. Finally, the model yields polar-angle response probabilities that can be used to calculate expectancy values of performance measures. More details about the model stages are described in Baumgartner *et al.* (2014).

### **Integration of auditory-periphery model**

In Baumgartner *et al.* (2014), we used a linear Gammatone filterbank and were able to predict several effects of HRTF modifications and spectral variations of the sound source on localisation performance. A more realistic model of the auditory periphery is required for modelling level dependencies and the effects of individual hearing impairment. Thus, in the present study, we replaced the Gammatone filterbank by the humanized auditory-periphery model from Zilany *et al.* (2009; 2014), in the following called the Zilany model. In order to obtain internal excitation patterns, we temporally integrated the instantaneous firing rates from the synapse output and then averaged the outputs across fibre types according to their physiologically assumed frequency of 61% high-, 23% medium-, and 16% low-SR fibres (Lieberman, 1978). Within the Zilany model, the frequency range from 0.7-18 kHz was represented by 100 auditory-nerve fibres, the internal sampling rate was 100 kHz, and the approximate implementation of the power-law functions was used.

### Listeners and stimuli

We simulated 14 female and nine male listeners aged between 19 and 46 years. Simulated stimuli were Gaussian white noise bursts with a duration of about 170 ms. Informal tests have shown that the excitation patterns differed only marginally for longer bursts. Targets were simulated in the midsagittal plane and polar angles between  $-30^\circ$  and  $270^\circ$ .

### Simulated conditions of hearing impairments

We simulated three degrees of OHC dysfunction and three conditions of SR-specific activity of AN fibres at SPLs of 50 dB and 80 dB in each case (see Table 1). Assuming perfect adaptation to the hearing impairment, model templates were processed according to the same OHC dysfunction and fibre types.

Factor	Levels	Meaning
COHC	COHC = 1.0	Intact OHC functionality
	COHC = 0.5	Moderate OHC dysfunction
	COHC = 0.1	Severe OHC dysfunction
FT	LMH	Activity of low-, medium-, and high-SR fibres
	MH	Activity of medium-, and high-SR fibres
	H	Activity of only high-SR fibres

**Table 1:** Simulated conditions of impaired auditory peripheries.

### Data analysis

Localisation performance was quantified by the following measures. The quadrant error rate (QER) is the percentage of polar-angle errors larger than  $90^\circ$ . The local polar error (LPE) is the root mean square (RMS) of polar-angle errors smaller than  $90^\circ$ . The polar gain is the slope of a linear regression line fitted separately to responses in the front and the rear hemispheres. Quasi-veridical responses are defined as responses deviating less than  $45^\circ$  from the regression line, and the variability is the RMS of deviations between quasi-veridical responses and the regression line.

In order to quantify the predictive power of the model, the following two metrics were used:  $e$  denotes the RMS difference between actual and predicted listener-specific performance measures, and  $r$  denotes Pearson's correlation coefficient between actual and predicted listener-specific performance measures.

For statical analysis of main effects, we performed 3-way repeated-measures analyses of variance (ANOVAs) with Greenhouse-Geisser correction for departure from sphericity. For post-hoc analysis, we used Tukey's honest significance difference test. All effects are reported as significant at  $p < .05$ .

## RESULTS AND DISCUSSION

### Model evaluation

First, we simulated three experimental conditions with moderate and approximately constant SPL from Baumgartner *et al.* (2014) and compared the predictive power of the new model with that from the Gammatone-based model. In order to reduce computational effort, simulations were only conducted for the median plane. Table 2 shows the results for a baseline condition testing localisation of Gaussian white noise bursts with reference HRTFs, a condition testing spectral warping of HRTFs in combination with band limitation (Majdak *et al.*, 2013), and a condition testing limited spectral resolution of HRTFs (Goupell *et al.*, 2010). Both model variants performed very similar, though the predictive power of the Gammatone-based model was slightly better in most cases.

Model of auditory periphery	Baseline				Warping				Resolution			
	QER (%)		LPE (deg)		QER (%)		LPE (deg)		QER (%)		LPE (deg)	
	<i>e</i>	<i>r</i>	<i>e</i>	<i>r</i>	<i>e</i>	<i>r</i>	<i>e</i>	<i>r</i>	<i>e</i>	<i>r</i>	<i>e</i>	<i>r</i>
Zilany	2.39	0.93	2.19	0.75	8.73	0.84	6.22	0.78	6.81	0.72	5.44	0.71
Gammatone	2.60	0.95	2.64	0.83	8.18	0.83	5.45	0.78	8.24	0.69	4.67	0.76

**Table 2:** Model performance for different approximations of the auditory periphery.

However, the Gammatone model cannot represent any SPL dependencies. In order to test the predictive power of the new model with respect to changes in SPL, we simulated the experiments from Sabin *et al.* (2005). Sabin *et al.* (2005) showed their results only as functions of the sensation level (SL), that is, the level relative to the detection threshold for a frontal target. For transferring our SPL-specific predictions to SLs, we generally assumed the SL to be 10 dB less than the SPL. Figure 1 shows the model predictions and the actual results replotted from Sabin *et al.* (2005). Predicted performance is more similar to the actual performance for the front than the rear. Especially in the front, the model predictions show a generally larger variability than the actual listeners from Sabin *et al.* (2005). The comparison of the quasi-veridical response rate for rear targets with an SL of less than 15 dB should be treated with caution because Sabin *et al.* (2005) considered a default regression line with a slope of one and intercept of 180° if less than five were audible and not confused between front and rear. In our simulations, we did not explicitly consider audibility and simulated many more trials. Hence, there were always enough responses to estimate a regression line.

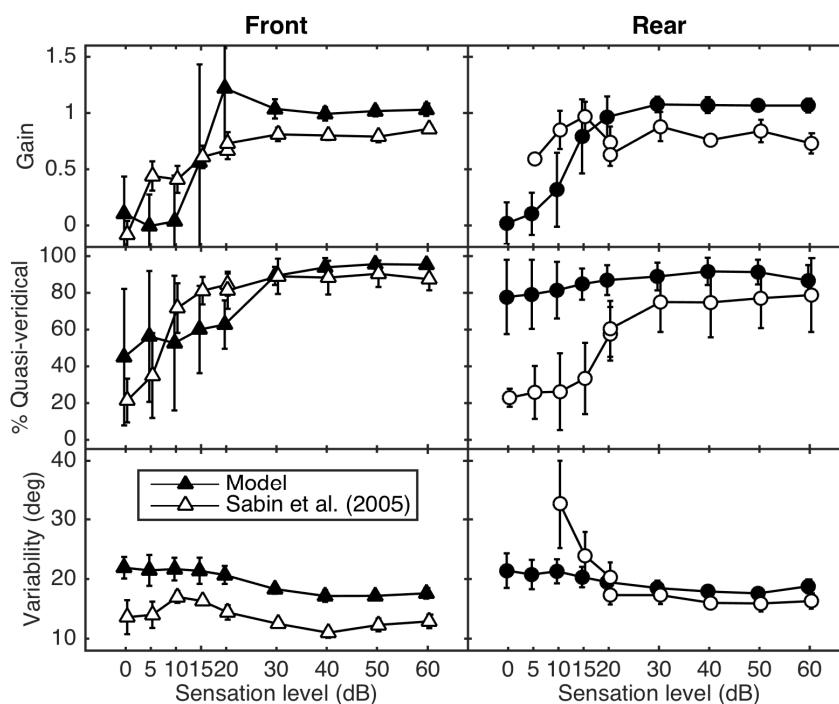


**Fig. 1:** Results of modelling the level dependence. Error bars represent standard deviations. The data are slightly shifted along the abscissa for better visibility. Results of two experimental blocks from Sabin *et al.* (2005) are shown at SL of 20 dB.

### Effects of OHC dysfunction and SR-specific loss of AN fibres

Predicted localisation performance for impaired auditory peripheries is shown in Fig. 2. There are significant main effects of the OHC dysfunction for QER [ $F(1.40,30.81) = 405.57$ ] and LPE [ $F(1.54,33.87) = 321.07$ ]. Paired comparisons revealed that QER and LPE are significantly larger for the severe dysfunction than for the moderate dysfunction and intact functionality. The moderate dysfunction and the intact functionality are not significantly different for QER but different for LPE. The main effects of fibre type activity (FT) are also significant for QER [ $F(1.92,42.19) = 840.74$ ], and LPE [ $F(1.25,27.51) = 691.76$ ]. In paired comparisons, all FT conditions are significantly different to each other. MH performed best, LMH slightly worse, and H worst. There is no significant main effect of the SPL for QER [ $F(1,22) = 0.78$ ], but LPE increases with SPL [ $F(1,22) = 13.46$ ]. There are significant interactions between OHC dysfunction and SPL both for QER [ $F(1.63,35.60) = 535.17$ ] and LPE [ $F(1.57,34.59) = 170.7$ ], as well as between OHC dysfunction and FT also both for QER [ $F(2.80,61.55) = 249.52$ ] and LPE [ $F(2.63,57.94) = 188.53$ ]. The QER and LPE degradation caused by severe OHC dysfunction is less severe for louder sounds and if only high-SR fibres are activated.

The ability of the AN fibre population to accurately represent spectral cues depends on the dynamic range they are able to capture. In order to obtain estimates of the

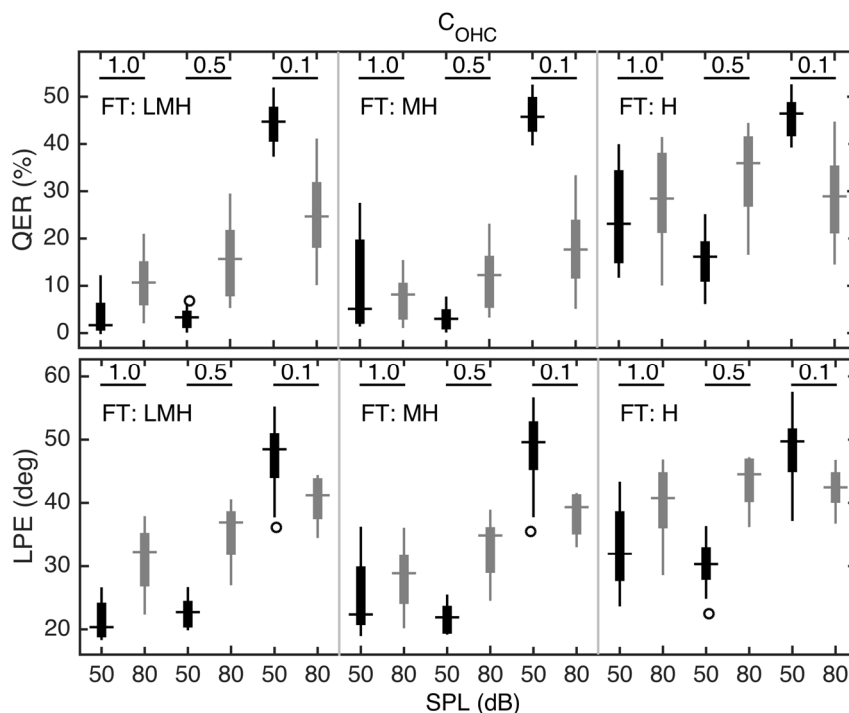


**Fig. 2:** Effects of OHC dysfunctions and SR-specific loss of AN fibres. Horizontal line: mean. Thick bar: interquartile range (IQR). Thin bar: data range within 1.5 IQR. Open circle: outlier.

dynamic ranges, we simulated AN responses to broadband noise at various SPLs in steps of 10 dB, averaged the predicted firing rates across the relevant frequency range between 700 Hz and 18 kHz, and finally differentiated these average rates across the SPL steps. The simulated rate differences are shown in Fig. 3 for the different fibre type combinations and degrees of OHC dysfunction. The range of rate differences being larger than zero indicates the dynamic range of the AN fibre population and the maximum rate difference indicates best sensitivity. Dynamic range bounds and sensitivity maxima are predicted to increase with OHC dysfunction. Within certain degrees of OHC dysfunction, predicted rate-difference curves are slightly shallower and peak at larger SPLs, the more fibre types are preserved. The consequently slightly larger dynamic range in the LMH and MH conditions compared to the H condition for the intact OHC functionality appears important to accurately represent the templates at 80 dB SPL with a level variability of at least 40 dB across frequencies and directions and thus explains that the model predicts degraded performance if only high-SR fibres are preserved. Very similar dynamic ranges but mostly higher sensitivities might be the reason for the slightly better performance in the MH condition compared to the LMH condition.

Localisation performance was shown to be relatively robust with respect to moderate OHC dysfunction, but, especially for silent sounds, a severe OHC dysfunction drastically degraded the performance. Figure 4 shows the positive spectral gradient profiles as functions of the polar angle for intact OHC functionality as well as moderate

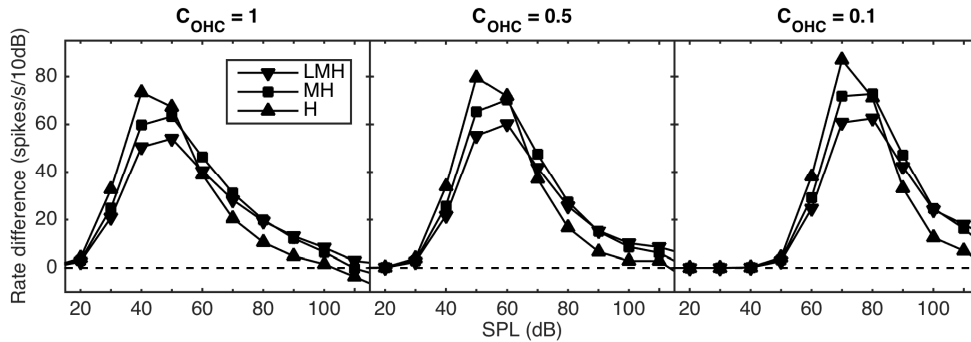


**Fig. 3:** Rate difference vs. level functions predicted for different combinations of fibre types and OHC dysfunctions. Frequency range: 0.7-18 kHz.

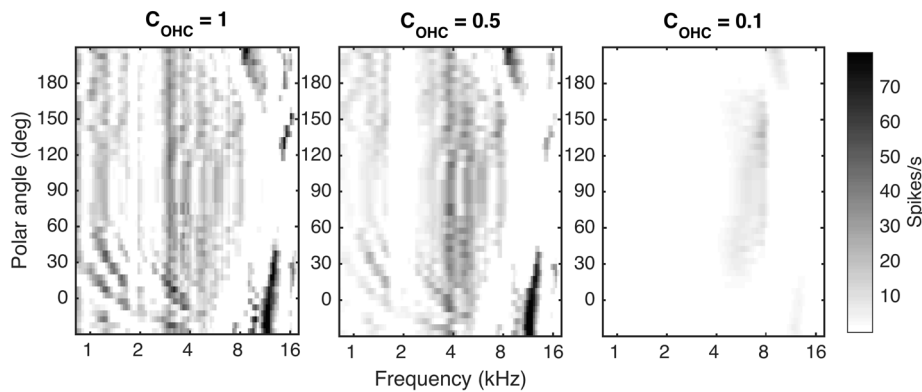


**Fig. 4:** Effect of OHC dysfunction on positive spectral gradients. Simulation for 50 dB SPL and all fibre types preserved (FT: LMH). Note that spectral gradients are almost absent for the most severe OHC dysfunction ( $C_{OHC} = 0.1$ ).

and severe OHC dysfunction from left to right. While the profiles for the intact and moderate cases are very similar and reveal direction-specific patterns, there are only very few and small gradients with little directionality in the severe case. In this severe condition, auditory filters are too broad to resolve most of the spectral information. Note that our investigations focussed on listening conditions without any background noise. The presence of background noise might increase the importance of proper OHC functionality (May *et al.*, 2004).

## CONCLUSIONS

In order to study the effect of peripheral hearing disorders on sound localisation in quiet in sagittal planes, we integrated the auditory periphery model from Zilany *et al.* (2009; 2014) into the sagittal-plane sound localisation model from Baumgartner *et al.* (2014). The initial model evaluation for normal-hearing listeners showed that replacing the Gammatone filterbank with the nonlinear Zilany model preserves the predictive power of the localisation model and enables level-dependent simulations. The model predicts poor localisation performance if only high-SR fibres are preserved in

the auditory periphery and low- and medium-SR fibres are lost because then the dynamic range of AN responses is too limited to represent HRTF-filtered sounds at various SPLs. Model predictions suggest that OHC dysfunctions are critical only if the dysfunction is quite severe. Moderate OHC dysfunctions seem to provide auditory filters sharp enough to capture spectral cues.

## ACKNOWLEDGMENTS

Thanks to Christian Kaseß for assistance with the statistical analyses.

## REFERENCES

- Baumgartner, R., Majdak, P., and Laback, B. (2014). "Modeling sound-source localization in sagittal planes for human listeners," *J. Acoust. Soc. Am.*, **136**, 791-802.
- Best, V., Carlile, S., Jin, C., and van Schaik, A. (2005). "The role of high frequencies in speech localization," *J. Acoust. Soc. Am.*, **118**, 353-363.
- Furman, A.C., Kujawa, S.G., and Liberman, M.C. (2013). "Noise-induced cochlear neuropathy is selective for fibers with low spontaneous rates," *J. Neurophysiol.*, **110**, 577-586.
- Goupell, M.J., Majdak, P., and Laback, B. (2010). "Median-plane sound localization as a function of the number of spectral channels using a channel vocoder," *J. Acoust. Soc. Am.*, **127**, 990-1001.
- Liberman, M.C. (1978). "Auditory-nerve response from cats raised in a low-noise chamber," *J. Acoust. Soc. Am.*, **63**, 442-455.
- Majdak, P., Walder, T., and Laback, B. (2013). "Effect of long-term training on sound localization performance with spectrally warped and band-limited head-related transfer functions," *J. Acoust. Soc. Am.*, **134**, 2148-2159.
- May, B.J., Budelis, J., and Niparko, J.K. (2004). "Behavioral studies of the olivocochlear efferent system: Learning to listen in noise," *Arch. Otolaryngol. Neck Surg.*, **130**, 660-664.
- Noble, W., Byrne, D., and Lepage, B. (1994). "Effects on sound localization of configuration and type of hearing impairment," *J. Acoust. Soc. Am.*, **95**, 992-1005.
- Otte, R.J., Agterberg, M.J.H., Wanrooij, M.M. V., Snik, A.F.M., and Opstal, A.J.V. (2013). "Age-related hearing loss and ear morphology affect vertical but not horizontal sound-localization performance," *J. Assoc. Res. Otolaryngol.*, **14**, 261-273.
- Rakerd, B., Vander Velde, T.J., and Hartmann, W.M. (1998). "Sound localization in the median sagittal plane by listeners with presbycusis," *J. Am. Acad. Audiol.*, **9**, 466-479.
- Reiss, L.A.J. and Young, E.D. (2005). "Spectral edge sensitivity in neural circuits of the dorsal cochlear nucleus," *J. Neurosci.*, **25**, 3680-3691.
- Sabin, A.T., Macpherson, E.A., and Middlebrooks, J.C. (2005). "Human sound localization at near-threshold levels," *Hear. Res.*, **199**, 124-134.
- Zilany, M.S.A., Bruce, I.C., Nelson, P.C., and Carney, L.H. (2009). "A phenomenological model of the synapse between the inner hair cell and auditory nerve: Long-term adaptation with power-law dynamics," *J. Acoust. Soc. Am.*, **126**, 2390-2412.
- Zilany, M.S.A., Bruce, I.C., and Carney, L.H. (2014). "Updated parameters and expanded simulation options for a model of the auditory periphery," *J. Acoust. Soc. Am.*, **135**, 283-286.